Evidence for frequency-dependent cortical plasticity in the human brain

Caroline A. Lea-Carnall[a,1], Nelson J. Trujillo-Barreto[a], Marcelo A. Montemurro[a], Wael El-Deredy[a,b,2], and Laura M. Parkes[a,2]

[a]Division of Neuroscience and Experimental Psychology, Faculty of Biology, Medicine and Health, University of Manchester, Manchester M13 9PL, United Kingdom; and [b]School of Biomedical Engineering, University of Valparaiso, Valparaiso 2366103, Chile

Edited by Peter Dayan, University College London, London, United Kingdom, and accepted by Editorial Board Member Marlene Behrmann June 29, 2017 (received for review December 31, 2016)

Frequency-dependent plasticity (FDP) describes adaptation at the synapse in response to stimulation at different frequencies. Its consequence on the structure and function of cortical networks is unknown. We tested whether cortical "resonance," favorable stimulation frequencies at which the sensory cortices respond maximally, influenced the impact of FDP on perception, functional topography, and connectivity of the primary somatosensory cortex using psychophysics and functional imaging (fMRI). We costimulated two digits on the hand synchronously at, above, or below the resonance frequency of the somatosensory cortex, and tested subjects' accuracy and speed on tactile localization before and after costimulation. More errors and slower response times followed costimulation at above- or below-resonance, respectively. Response times were faster after at-resonance costimulation. In the fMRI, the cortical representations of the two digits costimulated above-resonance shifted closer, potentially accounting for the poorer performance. Costimulation at-resonance did not shift the digit regions, but increased the functional coupling between them, potentially accounting for the improved response time. To relate these results to synaptic plasticity, we simulated a network of oscillators incorporating Hebbian learning. Two neighboring patches embedded in a cortical sheet, mimicking the two digit regions, were costimulated at different frequencies. Network activation outside the stimulated patches was greatest at above-resonance frequencies, reproducing the spread of digit representations seen with fMRI. Connection strengths within the patches increased following at-resonance costimulation, reproducing the increased fMRI connectivity. We show that FDP extends to the cortical level and is influenced by cortical resonance.

plasticity | fMRI | cortical resonance | somatosensory | neural mass model

Neuroplasticity refers to the brain's ability to modify its internal connections in response to external stimuli or following trauma, and underpins many cognitive processes involved in learning and memory formation across our life-span (1, 2). It is generally accepted that information in the brain is stored as patterns of connectivity (3) and therefore that the act of learning, whether achieved through passive stimulation or active engagement in a task, necessitates activity-dependent changes to network connectivity. This is accomplished by altering synaptic efficacy in response to external stimuli, and cellular-level studies have indicated that long-term potentiation (LTP) and long-term depression (LTD) are likely to underlie this process (4). LTP is defined as a strengthening of the synaptic connections; it was first described in the 1970s by Bliss and Lømo (5) in their groundbreaking work on hippocampal cells and has since been observed in many regions of the brain. Animal studies have shown that the frequency of synaptic activation modifies plasticity in both glutamatergic and GABAergic synapses (6–10), with reports that high- vs. low-frequency stimulation results in LTP or LTD, respectively (4). Although stimulation frequency appears to be an important factor in plasticity studies, the consequences of frequency-dependent cellular changes on the structure and function of cortical networks are unknown.

A recent study in humans found distinct frequency-dependent behavioral outcomes after tactile stimulation where low-frequency caused impaired performance, whereas high-frequency stimulation improved performance (11) (see refs. 12 and 13 for reviews of similar experiments). The primary somatosensory cortex (SI) also shows rapid topographic reorganization in response to repetitive sensory inputs (14–19). Of particular interest are the perceptual changes that accompany such reorganization. Tactile acuity improvements following tactile stimulation of a single digit over several hours coincide with increased cortical representation of the stimulated site within SI (16–19). Furthermore, synchronous costimulation of two digits has been shown to lead to shifting of the cortical representations of the digit regions toward one another and impaired discrimination performance after stimulation (14, 15). SI therefore appears to be an ideal test bed in which to study the impact of the frequency of repetitive stimulation on the plasticity of cortical networks, and associated behavior.

A missing factor in frequency-dependent plasticity (FDP) studies is the notion of resonance. Neurons, neural assemblies, and cortical networks all exhibit resonance characteristics, whereby they respond maximally to repetitive input within a

Significance

We extend the concept of frequency-dependent plasticity, thus far used to describe synaptic selective adaptation in response to stimulation at different frequencies, to the level of cortical networks. We demonstrate selective changes in perception, functional topography, and connectivity of the primary somatosensory cortex following tactile stimulation at different frequencies. Simulation of a network of oscillators incorporating Hebbian learning reproduced these changes and confirmed the influence of intrinsic cortical resonance on plasticity. We thus show that frequency-dependent plasticity extends to the cortical level and is influenced by cortical resonance, which is of potential importance for optimization of therapeutic stimulation approaches to augment learning and memory.

Author contributions: C.A.L.-C., N.J.T.-B., W.E.-D., and L.M.P. designed research; C.A.L.-C., M.A.M., and L.M.P. performed research; L.M.P. contributed new reagents/analytic tools; C.A.L.-C., N.J.T.-B., W.E.-D., and L.M.P. analyzed data; and C.A.L.-C., N.J.T.-B., M.A.M., W.E.-D., and L.M.P. wrote the paper.

The authors declare no conflict of interest.

This article is a PNAS Direct Submission. P.D. is a guest editor invited by the Editorial Board.

Data deposition: All fMRI data are available in the Zenodo repository, https://zenodo.org/ (DOI 10.5281/zenodo.399256).

[1]To whom correspondence should be addressed. Email: caroline.lea-2@postgrad.manchester.ac.uk.

[2]W.E.-D. and L.M.P. contributed equally to this work.

This article contains supporting information online at www.pnas.org/lookup/suppl/doi:10.1073/pnas.1620988114/-/DCSupplemental.

specific favored frequency range. For example, the human primary somatosensory cortex has a resonance frequency in the range of 20–26 Hz (20, 21). Cortical resonance is determined by both the biophysical properties of the individual neurons and the network connectivity architecture (22, 23); thus, stimulating a network near or far from its resonance frequency may result in different network behaviors, which could ultimately affect task performance. A recent computational paper investigating FDP found that the stimulation frequency responsible for inducing maximum LTP was related to axonal length (24), an anatomical feature of cells that is thought to affect resonance in neural circuits (25, 26). Given this, we wanted to examine the effect of repetitive tactile stimulation applied at a range of frequencies, at and away from resonance, on the plastic connectivity properties of the human primary somatosensory cortex.

We tested the effects of FDP on human performance and brain functional topography and connectivity of the primary somatosensory cortex using psychophysics and fMRI in separate studies. We applied repetitive tactile costimulation to two digits on the right hand at 7 Hz (below-resonance), 23 Hz (at-resonance), or 39 Hz (above-resonance), and tested subjects' performance on a standard tactile localization task before and after periods of costimulation. Using fMRI, we compared changes in digit region localization and functional connectivity between the regions before and after costimulation at-resonance and above-resonance. To relate the behavioral and imaging results to synaptic plasticity, we implemented a computational model using a network of Wilson–Cowan (WC) oscillators (27, 28) incorporating both Hebbian learning rules and homeostatic scaling mechanisms (29). We stimulated the model with a range of driving frequencies and tested the effect of frequency on the plastic connections, drawing comparisons with our experimental results. The term "frequency-dependent plasticity," has thus far been mostly used to describe the phenomenon at a cellular level. Here, we extend the concept of spike-timing–dependent plasticity to understanding the effects at the systems level and suggest that the phenomenon that starts at the level of the synapse has implications at the macro scale.

Results

Psychophysics: Frequency-Dependent Mislocalization Errors. The human primary somatosensory cortex is known to exhibit resonance characteristics in the range of 20–26 Hz. We stimulated digits 2 (D2) and 4 (D4) of the right hand simultaneously with a tactile stimulator at 7 Hz (below-resonance), 23 Hz (at-resonance), or 39 Hz (above-resonance) (*Materials and Methods*). We used a forced-choice tactile localization task to test mislocalization rates and reaction times before and after 20, 40, and 60 min of costimulation (Fig. 1).

Two-way repeated-measures ANOVA with factors session (pre/post) and driving frequency (below-resonance/at-resonance/above-resonance) was performed on the mislocalization scores obtained prestimulation and after 60 min of stimulation in R (version 3.1; R Foundation for Statistical Computing). We found no effect of frequency, a main effect of session ($P < 0.001$, $F = 12.3$) and an interaction between frequency and session ($P < 0.001$, $F = 8.5$). Mislocalization impairment (scores obtained after 60 min of costimulation compared with baseline) was significantly greater than zero following above-resonance stimulation only ($P < 0.00001$; difference, 9.73; 95% CI, 6.1, 13.4). Similar statistical analysis was performed for reaction times. We found no main effect of frequency or session but an interaction between frequency and session ($P = 0.003$; $F = 6.6$). Reaction times (after 60 min of costimulation compared with baseline) were significantly slower following below-resonance stimulation ($P = 0.006$; difference, 182 ms; 95% CI, 54 ms, 310 ms), and significantly faster following at-resonance stimulation ($P = 0.025$; difference, −156 ms; 95% CI, −292 ms, −21 ms).

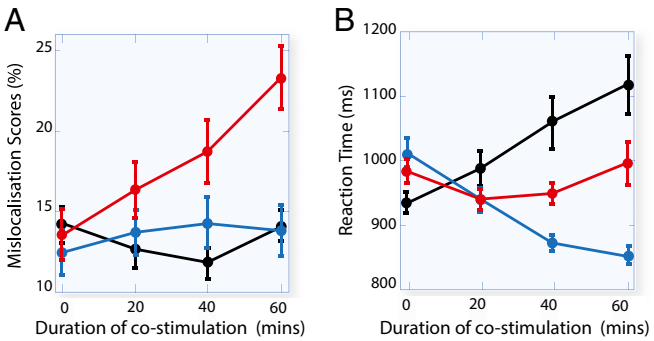

Fig. 1. Frequency-dependent mislocalization errors and reaction times in a tactile discrimination task during ongoing stimulation at the resonance frequency of the somatosensory cortex (23 Hz, blue), below-resonance (7 Hz, black), and above-resonance (39 Hz, red). Participants completed a forced-choice tactile discrimination task. Mean mislocalization (and SE) rates (*A*) and reaction times (*B*) at baseline and after three periods of 20 min of simultaneous continuous stimulation of D2 and D4 of the right hand at one of the three frequencies. Stimulation of the digits at the resonance frequency facilitated response time at no cost to performance accuracy, whereas stimulation above or below the resonance frequency either deteriorated performance or increased reaction times, respectively.

In summary, costimulation at the resonance frequency of the somatosensory cortex resulted in faster reaction times with no change in accuracy in the mislocalization test. In contrast, costimulation at the above-resonance or below-resonance frequency either deteriorated task performance or slowed down reaction times, respectively.

Imaging Results: Frequency-Dependent Functional Anatomy and Connectivity. To understand the changes in the functional anatomy and connectivity associated with observed behavioral changes, we repeated the experimental protocol during an fMRI session to test changes in the cortical representations of digits D2 and D4 before and after 46 min of costimulation. Both digit activation maps and functional connectivity changes were compared using the two driving frequencies "at-resonance" and "above-resonance." These two frequencies were chosen because we hypothesized that impaired mislocalization (found after costimulation above-resonance) and faster reaction times (observed after costimulation at-resonance) were a result of altered cortical topography and neuronal connectivity within SI. We calculated the Euclidean distance between the cortical maps for D2 and D4, as well as functional connectivity strength between the digit regions. The results of a mislocalization task (identical to that described in the previous section) administered before and after the scan confirmed the results found in the psychophysics experiment reported previously.

Digit separation. The mean distance between the center voxel of the cortical regions of D2 and D4 before and after the two stimulation frequencies is given in Fig. 2*A*. Following 23-Hz costimulation, there was a small decrease in the mean distance between the digit regions (0.73 mm; SE, 0.70 mm), whereas after costimulation at 39 Hz there is a greater reduction in digit separation (3.4 mm; SE, 1.19 mm). This size of reduction is in line with those seen in previous works (14, 15). A two-way repeated-measures ANOVA was performed on the digit separation distances with factors session (pre/post) and driving frequency (at-resonance/above-resonance). We found a trend for main effect of frequency ($P = 0.08$, $F = 3.4$), a main effect for session ($P = 0.01$; $F = 10.7$), and a trend for a session by frequency interaction effect ($P = 0.069$; $F = 3.8$). The difference between the digit regions (post compared with prestimulation) was significantly less than zero for the above-resonance only ($P = 0.003$; difference, −3.4 mm; 95% CI, −5.5 mm, −1.3 mm) suggesting that the digit representations shifted/expanded toward

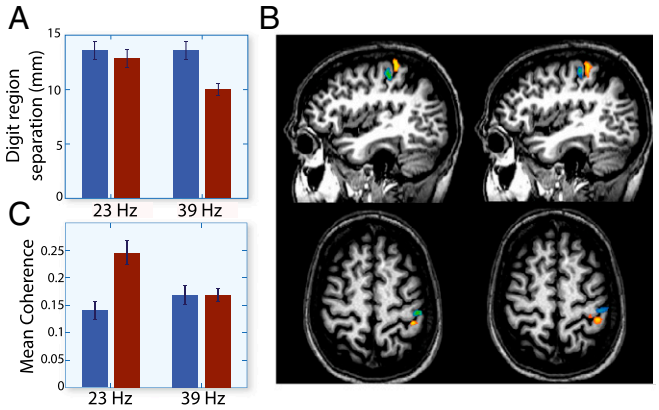

Fig. 2. FDP of digit region representations. (*A*) Digit separation. Mean distance between the cortical regions of digits D2 and D4 within SI before (blue) and after (red) costimulation at-resonance (23 Hz) and above-resonance (39 Hz) (n = 9); SE is given as bars. The distance between the maps reduced significantly after above-resonance costimulation, suggesting the digit regions merge closer together. (*B*) Functional imaging of a single participant. fMRI Image from a single participant indicating the digit regions for D2 (blue) and D4 (red), prestimulation (*Left*) and poststimulation (*Right*) with 39-Hz driving frequency in the sagittal and axial views. (*C*) Functional connectivity. Partial coherence averaged across all participants obtained between regions D2 and D4 for each of the four conditions; prestimulation (blue) and poststimulation (red) for both of the driving frequencies, 23 Hz (*Left*) and 39 Hz (*Right*) (n = 9); SE is given as bars. There is stronger functional coupling between the two digits following costimulation at 23 Hz.

one another in this case. The fMRI activation maps for a single participant indicating the digit regions for D2 (blue) and D4 (red) prestimulation (left) and poststimulation (right) with 39-Hz driving frequency in the sagittal and axial views is given in Fig. 2*B*.

Functional connectivity between the digit regions. We calculated partial coherence as a measure of functional connectivity (FC) between the digit regions per participant for each experimental condition (30). Fig. 2*C* shows the average coherence across all participants for each of the four conditions; prestimulation and poststimulation for both of the driving frequencies, 23 and 39 Hz. After stimulation with at-resonance driving frequency (23 Hz), FC is increased between the digit regions (prestimulation, 0.13; SE, 0.02; poststimulation, 0.24; SE, 0.02), whereas no change is observed in FC after stimulation at above-resonance driving frequency (39 Hz) (prestimulation, 0.17, SE 0.03; poststimulation, 0.17, SE 0.02).

A two-way repeated ANOVA with factors session (pre/post) and driving frequency (at-resonance/above-resonance) was performed on the FC values. We found a trend toward an effect of session ($P = 0.07$; $F = 4.4$), no effect of frequency, and a significant session by frequency interaction ($P = 0.036$; $F = 5.2$). FC difference (postpre) was significantly greater than zero following at-resonance only ($P = 0.007$; difference, 0.10; 95% CI, 0.03, 0.17).

In summary, stimulation at the resonance frequency of the somatosensory cortex resulted in strong functional connectivity, without any change in functional anatomy. In contrast, stimulation at the above-resonance frequency merged the cortical maps of the two stimulated digits but did not change functional connectivity between them.

Computational Results: Frequency-Dependent Hebbian Network Formation. To link the psychophysics and imaging results to the reported data at the cellular and molecular level on FDP (3–5, 8, 31), we implemented a simulation of the experiment in an adaptive neuronal network model of coupled oscillators. Our aim was to investigate whether network connections are frequency dependent. A network model of loosely coupled WC oscillators (27, 28) was implemented with resonance ≈15 Hz. Excitatory connections between the units were designed to exhibit Hebbian plasticity (see *Materials and Methods* for details of the learning rule), and inputs to all units (excitatory and inhibitory) were subject to homeostatic scaling, a mechanism by which individual neuronal units can modulate their incoming activity via their own subcellular structures (32). Two circular patches of size of 156 units (radius, 350 μm) embedded in a 50 × 50 network of loosely coupled WC oscillators (Fig. 3*A*) were costimulated with external driving frequencies between 5 and 50 Hz.

Propagation of the signal through the network. We measured propagation of the driving frequency from the activated patches to the rest of the network by calculating the proportion of units outside the stimulated patches activated above baseline at each frequency (*Materials and Methods*).

The relative power (compared with a network driven by white noise) of each unit in the network in response to below- or above-resonance stimulation of the two patches (dark red) is shown in Fig. 3*B*. The proportion of units external to the activated patches that were activated by each of the driving frequencies is shown in Fig. 3*C*. Driving frequencies below the network resonance frequency (≈15 Hz) do not propagate. Stimulation propagates through the network as the frequency of stimulation increases above the resonance frequency.

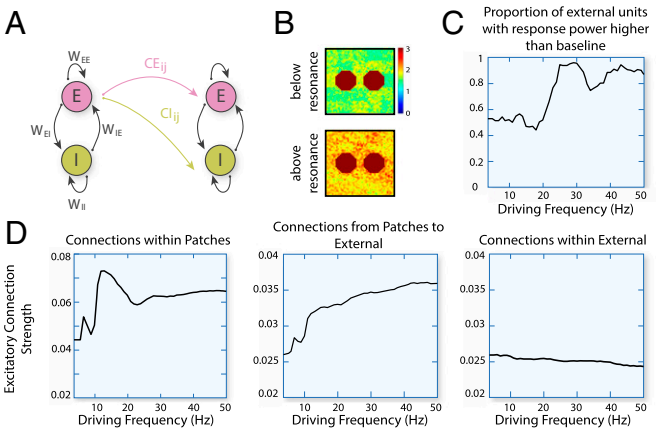

Fig. 3. Computational results. (*A*) Schematic diagram of the WC model. Two units are shown, both containing an excitatory (*E*) and an inhibitory (*I*) population, the parameters W_{EE}, W_{EI}, W_{IE}, and W_{II} describe connectivity within a single unit. Interunit connectivity is governed by the connectivity matrices *CE* and *CI*. Input to units is subject to homeostatic scaling (*Materials and Methods*). (*B*) Response power of each unit relative to baseline power for two driving frequencies. The response power of each unit within the network relative to the power of the same frequency for a network driven by white noise only is given for two driving frequencies: below-resonance (8 Hz, *Top*) and above-resonance (26 Hz, *Bottom*) applied to the two activated patches (dark red). The scale has been reduced to show the increased power around the edges and especially around and in-between the activated regions. (*C*) Proportion of external units with response power higher than baseline, indicating signal propagation. The proportion of units within the network that were external to the activated patches that had response power significantly greater than baseline is given for each of the driving frequencies calculated using the nonparametric Kruskal–Wallis test. It can be seen that propagation is low for driving frequencies lower than the resonance frequency of the network (≈15 Hz). For driving frequencies above 25 Hz, the signal has propagated to almost the entire network in many cases. This indicates that propagation of the stimulus to neighboring units is also frequency dependent. (*D*) Connectivity strength within the network as a function of driving frequency. Mean final connection strength for connections between units inside the stimulated patches (*Left*) shows maximal connectivity for driving frequency at ≈15 Hz, the resonance of simulated network. Connections between units inside the stimulated patch and units outside the patch (*Middle*) show maximal connectivity strengths when stimulated above the resonance frequency. Connections that neither originate in nor target the activated patch (*Right*) act as a control, and it can be seen that they are unaffected by stimulus frequency.

Evolution of excitatory connections within the network. We evaluated connection strengths for every pair of units in the network at each driving frequency. There are three types of connections: between units within the stimulated patches (Fig. 3*D*, *Left*); between units within to outside (Fig. 3*D*, *Middle*); and between units outside the patches (Fig. 3*D*, *Right*). Connection strengths between units inside the patches were maximal when the stimulation frequency was close to the resonance frequency of the network. This result mirrors the increase in functional connectivity that was observed in the fMRI data previously (Fig. 2*C*) and may account for the faster response time in the behavioral data. Connection strengths between units inside to outside the stimulated patch increased with increasing driving frequency. This mirrors the expansion of the digit representations observed in the fMRI, and may account for the poor performance observed in the psychophysics test. Connection strengths between units outside the stimulated patch were unaffected by stimulation frequency.

In summary, these findings indicate that, in our model, there is a frequency dependence of the connectivity strengths.

Discussion

In this study, we combined psychophysics, neuroimaging, and neurocomputational modeling to better understand the neural changes underlying FDP. We used an established method of digit costimulation (33) to induce plasticity in the human primary somatosensory cortex. We observed that plastic changes were not only modulated by the driving frequency of stimulation, but also depended on whether this frequency was at, above, or below the resonance frequency of the primary somatosensory cortex (20–26 Hz) (20, 21).

Initially, the influence of frequency-specific stimulation on perceptual discrimination was tested by costimulation of digits D2 and D4 at one of the three driving frequencies for 1 h. We found that costimulation above-resonance substantially impaired the ability to localize stimuli to one of the digits, probably due to a spreading, expanding, or shifting of the digit representations within SI, a process that has previously been shown to correlate with the observed perceptual changes (15). In contrast, costimulation at-resonance did not affect mislocalization, but participants were significantly faster. We hypothesized that, close to its resonance frequency, there is a strengthening of the synapses within the stimulated region, resulting in greater efficiency in the Hebbian sense. Costimulation below-resonance did not significantly affect performance but slowed reaction times, perhaps reflecting fatigue, and indicating that plastic changes were minimal in this condition (Fig. 1).

To validate this interpretation, we performed fMRI before and immediately following 46 min of the same costimulation paradigm using the two driving frequencies at- and above-resonance as both of these cases resulted in a significant change to either performance or reaction time, which we hypothesized was attributable to measurable plastic change within SI. We confirmed that the digit regions shift/expand following above-resonance costimulation and result in a reduced separation of their center voxel. Previous studies using similar experimental protocols but using non-continuous costimulation over a longer period (3 h) reported digit shifts comparable to ours and in one case reported that these were associated with worsening task performance (14–16). We also confirmed an increase in functional connectivity between the digit regions following the at-resonance costimulation, which was not observed for the above-resonance case.

Given that much of the prior work on FDP is carried out at the microscopic scale, we set out to link our macroscopic psychophysics and imaging observations to previous reports using computational modeling. We implemented a network model of loosely coupled WC oscillators with plastic Hebbian connections to further understand the experimental findings. We selectively stimulated two small patches within the network at a range of driving frequencies and observed the effect on signal propagation and connectivity strength within the stimulated patches and throughout the network. We found that connections in the model behaved differently according to whether they were connecting units inside the patches (Fig. 3*D*, *Left*), or units inside the patches to units outside (Fig. 3*D*, *Middle*), or only connecting units outside the patches (Fig. 3*D*, *Right*). Specifically, we found (*i*) the highest excitatory connection strengths occurred within the patches when driven at close to the resonance frequency and (*ii*) that propagation of the signal was strongest following stimulation above the resonance frequency (Fig. 3 *B* and *C*). Driving the network at frequencies below its resonance resulted in excitatory connection strengths that were weaker than in the other two conditions and this applied to connections both between network units within the stimulated patches as well as units from the patches to outside. As a result, there was also less propagation of the driving signal across the network (Fig. 3 *B* and *C*).

To summarize, we found that at-resonance costimulation strengthened functional connectivity between the digit regions and speeded up reaction times. Modeling work supported the observations in that the greatest connection strengths within the stimulated patches occurred in this regime. Above-resonance costimulation impaired performance, but did not affect reaction times. Neuroimaging showed no change in FC between the digit regions but indicated that the digit regions had shifted or expanded closer together. Modeling results supported these findings in that connections from the patches to external regions (and therefore signal propagation) were greatest at higher frequencies. Previous experimental work has also shown that repetitively paired presynaptic and postsynaptic spikes at low interstimulus intervals result in greater synaptic modification than for larger intervals (34). Below-resonance costimulation did not affect performance but slowed reaction times. Evidence from our modeling work indicated that, at lower stimulation frequencies, connectivity within the activated patches, and from the patch to external regions, was lower than the two other stimulus conditions.

Although we do not account explicitly for plasticity of the inhibitory connections in our model, these results indicate that inhibitory processes at the border of the activated patch may be strengthened maximally during costimulation at-resonance, preventing the digit regions from expanding or shifting, which would result in impaired performance of the mislocalization task. There is evidence that during low-frequency stimulation GABA activity restricts excitatory synaptic potentiation, whereas at higher frequencies, the inhibitory connections are weakened (10). This phenomenon may account for the movement of the digit regions and the deterioration in performance that we observed following above-resonance stimulation. In future work, perhaps with higher resolution imaging at higher field strength, it would be interesting to determine whether the observed shift in digit regions is driven by the voxels that respond most strongly to the stimuli, or those with a weaker response, on the edge of the digit regions, corresponding to more subthreshold activity. Previous studies have found increased coherence between neural regions correlates with faster reaction times (35), which may account for the behavioral changes observed following at-resonance stimulation. It has been suggested that increased coherence allows optimal processing of stimulus input due to synchronized timing of the ongoing neural activity (see ref. 36 for a review). Inclusion of reaction time mechanisms and plastic inhibitory connections are areas for further model development.

The nature of our costimulation (continuous repetitive stimulation at fixed frequency) is somewhat different from what has been used in previous work. The majority of studies use intermittent synchronous stimulation at ≈1 Hz (15, 18, 19, 37), making it difficult to draw comparisons with our study. However, overall, these studies show synchronous stimulation leads to improved two-point discrimination on the stimulated digits, yet increased mislocalization between costimulated digits. It is suggested

(37) that this is due to an enlargement of cortical representations (leading to poorer localization), yet also a strengthening of connections within those representations (leading to improved two-point discrimination). Our results support this notion, in so much that we see spreading of representations underlying poorer mislocalization (at above-resonance frequencies), yet stronger connections within regions leading to faster reaction times (at-resonance). It would be informative to see whether at-resonance continuous stimulation improves two-point discrimination on a single digit, as would be predicted by the model. Work by Ragert et al. (11) used pulsed stimulation at 20 Hz (1-s stimulation every 5 s) and found improved two-point spatial discrimination, but neither mislocalization nor reaction time was reported, again making it hard to draw comparisons with our work. It would be interesting to consider the impact of asynchronous stimulation on our test system. Our previous work (14) shows that asynchronous stimulation results in digit separation, with similar results reported in other human (15) and animal studies (38), and so and it might be predicted that this would also be the case here. It is also important to note that, although we apply peripheral stimulation, there is abundant evidence from the somatosensory steady-state response literature (20) that the temporal structure of the stimulation will be reproduced in the cortex.

Hebbian learning is thought to underlie many forms of memory formation and learning (39). In our model, we developed a Hebbian learning rule, designed to use proportional firing rates as its input so as to be suitable for use with a neural mass model that does not output spikes explicitly. In addition, input to each cell was modulated via homeostatic scaling (29). In this way, units can modulate their excitation levels allowing them to remain within suitable limits such that they are optimally responsive to their dynamic synaptic input levels (40), and remain stable. Other mechanisms of plasticity include LTD (41) and short-term potentiation (42); however, these were not included in the current model to simplify the calculations. The inclusion of all these biological processes is also an area for future model development.

FDP has already been shown to occur in various animal models (3, 5, 31). Inhibitory GABAergic interneurons appear to underlie this frequency dependence by hyperpolarizing postsynaptic neurons during low-frequency stimulation prohibiting glutamate binding and synaptic potentiation (43). At higher driving frequencies, GABA release is decreased, allowing synaptic potentiation to occur (10). Pioneering work by Markram and Tsodyks (44) describes the frequency dependence of signal potentiation in the rat somatosensory cortex. They found that the boundary between potentiation and depression was dependent on properties of the synapses such as recovery rates (45). These same synaptic properties are also thought to be responsible for the resonance properties of cells (23), and therefore high and low frequency are themselves relative terms, dependent on the cell's intrinsic properties. In this work, we attempt to provide a context to better understand high- and low-frequency stimulation in relationship to the resonance of the sensory systems under investigation. Indeed, we find a clear effect of stimulation frequency on cortical plasticity, with different behavioral and imaging outcomes depending on whether the stimulation is above-, at-, or below-resonance. This behavior may be grounded in the frequency dependence of LTP, but further work is required to improve our understanding of the potential equivalence of these phenomena.

In conclusion, by combining three separate experimental modalities—psychophysics, MR imaging, and computational modeling—we have been able to interrogate this simple model of plasticity in humans. Translation of these key ideas to more complex methods of stimulation would be of great interest. In this paper, we have shown that the frequency of stimulation is crucial to consider when designing protocols aimed at inducing plasticity. For example, in cases where increased performance of a task that has already been learned is required, then we may want to present the stimuli at the resonance frequency of the system, such as improving motor or language skills after stroke. Alternatively, if remapping of the network topography is the aim, to overcome phantom limb pain for example, then stimulation of adjacent regions using above-resonance driving frequency would be optimal. Finally, it is important to note that we measured changes in cortical organization and connectivity in a single scanning session, which could be key for clinical applications where assessment of the propensity of the brain to undergo plastic change could be of relevance, for example in stroke or dementia. If it is possible to probe synaptic plasticity in a single session, then there is greater potential for it to be used as a marker or predictor of neurological decline or treatment response.

Materials and Methods

This study was approved by the University of Manchester Ethics Committee, and fully informed written consent was obtained from all subjects before participation. For full details of the experimental procedure and analysis methods, please see *SI Materials and Methods*.

Psychophysics. Forty-five healthy right-handed subjects were recruited from the student/staff population (nine participants repeated two of the conditions, resulting in 54 datasets). Participants were assigned to either the 7-Hz ($n = 19$), 23-Hz ($n = 17$), or 39-Hz ($n = 18$) condition. We initially determined participants' sensory threshold of digits D2 and D4 of the right hand using the Presentation system (Neurobehavioral Systems; www.neurobs.com/). Participants then completed a mislocalization test; a two-alternative forced-choice test where subjects had to respond as to which of the two digits had been stimulated, to measure baseline mislocalization rate. Following this, the two digits were synchronously costimulated for three periods of 20 min at one of three driving frequencies. Stimulators were driven using Matlab software (www.mathworks.com) that constructed a sine wave with the desired frequency (7, 23, or 39 Hz) delivered in-phase to each digit. Every 20 min (until a total of 60 min of stimulation was complete), the subjects' completed a further mislocalization test.

fMRI. MR data were acquired using a Philips 3-T Achieva system and an eight-channel phased array head coil for signal detection. Ten healthy right-handed subjects were recruited from the student/staff population (five males). Participants attended two separate identical scanning sessions separated by at least 14 d. The scan protocol consisted of a high-resolution T_1-weighted structural image and a baseline fMRI digit localization scan. These were followed by 46 min of additional scanning (results not reported here) while digits D2 and D4 of the subject's right hand received constant synchronous costimulation at either one of the two stimulation frequencies (23/39 Hz) and a final fMRI digit localization scan. In addition to this, participants completed a mislocalization test immediately before and following the scan.

Computational Modeling. In this study, we used the WC model as the basic unit of our network (27, 28). The network model we use has been described in detail previously (22); full details are given in *SI Materials and Methods*, but descriptions of the learning rule and simulations are given here.

The WC network model. The WC equations describe a single unit intended to represent a cortical minicolumn approximately 50 μm^2 in size. Units were fixed onto a 2D lattice with periodic boundary conditions to represent a small patch of cortical sheet. All excitatory connections within the network are plastic and evolve according to a Hebbian learning rule. In addition, inputs to all units are subject to homeostatic scaling using methodology developed by Remme and Wadman (29).

Hebbian learning within the model. Hebbian plasticity in the model is implemented through Eq. **1**, which specifies the dynamics of the excitatory connectivity matrix CE. In particular, in the absence of activity from units i and j (that is $E_i = E_j = 0$), or if the product of the firing rates from units i and j is lower than the threshold h, the matrix element CE_{ij} will decay toward zero. Otherwise, if both units are active with the product of the rates E_i and E_j above the threshold h, then then there is a positive contribution to the rate of change of CE_{ij} and the synapse is enhanced. The nonlinear threshold is implemented by the Heaviside function $\theta(x)$, which is zero for $x \leq 0$ and 1 otherwise:

$$\tau_h \frac{dCE_{ij}}{dt} = -CE_{ij} + \gamma E_i E_j \theta(E_i E_j - h). \quad [1]$$

Parameters for the plasticity equations are defined as follows: $\tau_h = 2.5$ s, $\gamma = 1$, and $h = 0.04$. The parameter h was chosen as the square of the mean firing

rate for the excitatory population in response to white noise. Therefore, in order for the connectivity to increase between two units, at least 50% of the excitatory population of each unit must be firing; the parameters τ_h, γ were chosen so that the slope of the decay (when the two units were not coincidently firing) was equal to that of the increase.

Simulations.

Propagation of the signal through the network. We generated a network consisting of 50×50 identical units with parameters and connectivity profiles as described above. Two circular subnetworks (size, 156 units each; radius, 350 μm) within this network were stimulated with a range of driving frequencies between 5 and 50 Hz in steps of 1 Hz. We generated 100 trials consisting of 30,000 time steps for each condition, as this was the length of time needed for the plastic excitatory connectivity strengths to stabilize. A mean power series was calculated from the squared complex conjugate of the Fourier coefficients, and normalized by the total area under the curve for each unit across all trials. The response power at the driving frequency was recorded per unit per trial, and this was then compared with the power of the same unit, calculated in the same way, in response to white-noise input only. The response power for each of two driving frequencies, 8 and 26 Hz, was calculated per unit and given relative to the power of the same frequency in response to white noise. We used the nonparametric Kruskal–Wallis test to determine whether the response power at the driving frequency was significantly higher than the power of that frequency at baseline.

Evolution of excitatory connectivity within the network. The excitatory connection strength between each coupled pair was classified according to whether it connected units within the patches, units from inside to outside the patches, or units outside of the patches. The final connection strength recorded at the end of each trial was averaged over trials per condition and connection type.

ACKNOWLEDGMENTS. We thank Barry Whitnall and the radiologists at Salford Royal National Health Service Foundation Trust, Karen Lopez, and Daniel Wand. C.A.L.-C. is funded by a doctoral training award from the Engineering and Physical Sciences Research Council (EPSRC). N.J.T.-B. is also funded by EPSRC Grant EP/N006771/1. W.E.-D. is funded by the Comisión Nacional de Investigación Científica y Tecnológica, Chile, Projects Fondo Nacional de Desarrollo Científico y Tecnológico 1161378 and Basal FB0008.

1. Wieloch T, Nikolich K (2006) Mechanisms of neural plasticity following brain injury. *Curr Opin Neurobiol* 16:258–264.
2. Nelson CA (1999) Neural plasticity and human development. *Curr Dir Psychol Sci* 8:42–45.
3. Bliss TV, Collingridge GL (1993) A synaptic model of memory: Long-term potentiation in the hippocampus. *Nature* 361:31–39.
4. Malenka RC, Bear MF (2004) LTP and LTD: An embarrassment of riches. *Neuron* 44:5–21.
5. Bliss TV, Lømo T (1973) Long-lasting potentiation of synaptic transmission in the dentate area of the anaesthetized rabbit following stimulation of the perforant path. *J Physiol* 232:331–356.
6. Xu C, Zhao MX, Poo MM, Zhang XH (2008) $GABA_B$ receptor activation mediates frequency-dependent plasticity of developing GABAergic synapses. *Nat Neurosci* 11: 1410–1418.
7. Hopkins WF, Johnston D (1984) Frequency-dependent noradrenergic modulation of long-term potentiation in the hippocampus. *Science* 226:350–352.
8. Caporale N, Dan Y (2008) Spike timing-dependent plasticity: A Hebbian learning rule. *Annu Rev Neurosci* 31:25–46.
9. Gaiarsa JL, Caillard O, Ben-Ari Y (2002) Long-term plasticity at GABAergic and glycinergic synapses: Mechanisms and functional significance. *Trends Neurosci* 25:564–570.
10. Davies CH, Starkey SJ, Pozza MF, Collingridge GL (1991) GABA autoreceptors regulate the induction of LTP. *Nature* 349:609–611.
11. Ragert P, Kalisch T, Bliem B, Franzkowiak S, Dinse HR (2008) Differential effects of tactile high- and low-frequency stimulation on tactile discrimination in human subjects. *BMC Neurosci* 9:9.
12. Parianen Lesemann FH, Reuter EM, Godde B (2015) Tactile stimulation interventions: Influence of stimulation parameters on sensorimotor behavior and neurophysiological correlates in healthy and clinical samples. *Neurosci Biobehav Rev* 51:126–137.
13. Beste C, Dinse HR (2013) Learning without training. *Curr Biol* 23:R489–R499.
14. Vidyasagar R, Folger SE, Parkes LM (2014) Re-wiring the brain: Increased functional connectivity within primary somatosensory cortex following synchronous co-activation. *Neuroimage* 92:19–26.
15. Pilz K, Veit R, Braun C, Godde B (2004) Effects of co-activation on cortical organization and discrimination performance. *Neuroreport* 15:2669–2672.
16. Pleger B, et al. (2001) Shifts in cortical representations predict human discrimination improvement. *Proc Natl Acad Sci USA* 98:12255–12260.
17. Pleger B, et al. (2003) Functional imaging of perceptual learning in human primary and secondary somatosensory cortex. *Neuron* 40:643–653.
18. Hodzic A, Veit R, Karim AA, Erb M, Godde B (2004) Improvement and decline in tactile discrimination behavior after cortical plasticity induced by passive tactile coactivation. *J Neurosci* 24:442–446.
19. Godde B, Ehrhardt J, Braun C (2003) Behavioral significance of input-dependent plasticity of human somatosensory cortex. *Neuroreport* 14:543–546.
20. Snyder AZ (1992) Steady-state vibration evoked potentials: Descriptions of technique and characterization of responses. *Electroencephalogr Clin Neurophysiol* 84:257–268.
21. Tobimatsu S, Zhang YM, Kato M (1999) Steady-state vibration somatosensory evoked potentials: Physiological characteristics and tuning function. *Clin Neurophysiol* 110: 1953–1958.
22. Lea-Carnall CA, Montemurro MA, Trujillo-Barreto NJ, Parkes LM, El-Deredy W (2016) Cortical resonance frequencies emerge from network size and connectivity. *PLoS Comput Biol* 12:e1004740.
23. Hutcheon B, Yarom Y (2000) Resonance, oscillation and the intrinsic frequency preferences of neurons. *Trends Neurosci* 23:216–222.
24. Kumar A, Mehta MR (2011) Frequency-dependent changes in NMDAR-dependent synaptic plasticity. *Front Comput Neurosci* 5:38.
25. Silberstein RB (1995) Neuromodulation of neocortical dynamics. *Neocortical Dynamics and Human EEG Rhythms*, ed Nunez PL (Oxford Univ Press, New York), pp 591–627.
26. Nunez PL, Srinivasan R, Fields RD (2015) EEG functional connectivity, axon delays and white matter disease. *Clin Neurophysiol* 126:110–120.
27. Wilson HR, Cowan JD (1972) Excitatory and inhibitory interactions in localized populations of model neurons. *Biophys J* 12:1–24.
28. Wilson HR, Cowan JD (1973) A mathematical theory of the functional dynamics of cortical and thalamic nervous tissue. *Kybernetik* 13:55–80.
29. Remme MWH, Wadman WJ (2012) Homeostatic scaling of excitability in recurrent neural networks. *PLoS Comput Biol* 8:e1002494.
30. Sun FT, Miller LM, D'Esposito M (2004) Measuring interregional functional connectivity using coherence and partial coherence analyses of fMRI data. *Neuroimage* 21:647–658.
31. Markram H, Gupta A, Uziel A, Wang Y, Tsodyks M (1998) Information processing with frequency-dependent synaptic connections. *Neurobiol Learn Mem* 70:101–112.
32. Chen N, Chen X, Wang JH (2008) Homeostasis established by coordination of subcellular compartment plasticity improves spike encoding. *J Cell Sci* 121:2961–2971.
33. Godde B, Stauffenberg B, Spengler F, Dinse HR (2000) Tactile coactivation-induced changes in spatial discrimination performance. *J Neurosci* 20:1597–1604.
34. Dan Y, Poo MM (2006) Spike timing-dependent plasticity: From synapse to perception. *Physiol Rev* 86:1033–1048.
35. Schoffelen JM, Oostenveld R, Fries P (2005) Neuronal coherence as a mechanism of effective corticospinal interaction. *Science* 308:111–113.
36. Womelsdorf T, Fries P (2006) Neuronal coherence during selective attentional processing and sensory-motor integration. *J Physiol Paris* 100:182–193.
37. Kalisch T, Tegenthoff M, Dinse HR (2007) Differential effects of synchronous and asynchronous multifinger coactivation on human tactile performance. *BMC Neurosci* 8:58.
38. Wang X, Merzenich MM, Sameshima K, Jenkins WM (1995) Remodelling of hand representation in adult cortex determined by timing of tactile stimulation. *Nature* 378:71–75.
39. Hebb DO (1949) *The Organization of Behavior: A Neuropsychological Theory*, A Wiley Book in Clinical Psychology (Wiley, New York).
40. Pérez-Otaño I, Ehlers MD (2005) Homeostatic plasticity and NMDA receptor trafficking. *Trends Neurosci* 28:229–238.
41. Bear MF, Abraham WC (1996) Long-term depression in hippocampus. *Annu Rev Neurosci* 19:437–462.
42. Erickson MA, Maramara LA, Lisman J (2010) A single brief burst induces GluR1-dependent associative short-term potentiation: A potential mechanism for short-term memory. *J Cogn Neurosci* 22:2530–2540.
43. Herron CE, Lester RA, Coan EJ, Collingridge GL (1986) Frequency-dependent involvement of NMDA receptors in the hippocampus: A novel synaptic mechanism. *Nature* 322:265–268.
44. Markram H, Tsodyks M (1996) Redistribution of synaptic efficacy between neocortical pyramidal neurons. *Nature* 382:807–810.
45. Okatan M, Grossberg S (2000) Frequency-dependent synaptic potentiation, depression and spike timing induced by Hebbian pairing in cortical pyramidal neurons. *Neural Netw* 13:699–708.
46. Vidyasagar R, Parkes LM (2011) Reproducibility of functional MRI localization within the human somatosensory cortex. *J Magn Reson Imaging* 34:1439–1444.
47. Wang Y, Goodfellow M, Taylor PN, Baier G (2012) Phase space approach for modeling of epileptic dynamics. *Phys Rev E Stat Nonlin Soft Matter Phys* 85:061918.
48. Wang Y (2013) Multi-scale modelling of epileptic seizure rhythms as spatio-temporal patterns. PhD thesis (University of Manchester, Manchester, UK).
49. David O, Friston KJ (2003) A neural mass model for MEG/EEG: Coupling and neuronal dynamics. *Neuroimage* 20:1743–1755.
50. Wang Y, Goodfellow M, Taylor PN, Baier G (2014) Dynamic mechanisms of neocortical focal seizure onset. *PLoS Comput Biol* 10:e1003787.
51. Voges N, Schüz A, Aertsen A, Rotter S (2010) A modeler's view on the spatial structure of intrinsic horizontal connectivity in the neocortex. *Prog Neurobiol* 92:277–292.
52. Jansen BH, Rit VG (1995) Electroencephalogram and visual evoked potential generation in a mathematical model of coupled cortical columns. *Biol Cybern* 73:357–366.
53. Jansen BH, Zouridakis G, Brandt ME (1993) A neurophysiologically-based mathematical model of flash visual evoked potentials. *Biol Cybern* 68:275–283.